

Spacecraft Charging Anomaly on a Low-Altitude Satellite in an Aurora

P. C. Anderson* and H. C. Koons†

The Aerospace Corporation, Los Angeles, California 90009

On May 5, 1995, the microwave imager instrument aboard the Defense Meteorological Satellite Program F13 spacecraft experienced a lockup of its microprocessor unit. The anomaly is attributed to an electrical malfunction caused by an electrostatic discharge on the vehicle. It occurred during an intense energetic electron precipitation event within a region of very low plasma density in the auroral zone. Plasma measurements indicate that the spacecraft frame charged to a voltage near 459 V within a few seconds. Calculations of the capacitance of the ungrounded thermal blankets covering the surface of the spacecraft are consistent with a surface charging time of a few seconds to reach several kilovolts. Subsequent electrostatic discharge led to the lockup.

Nomenclature

A	= area
C	= capacitance
i	= current density
R	= energy loss rate
t	= time
V	= voltage
δ	= secondary electron yield
ρ	= density

Introduction

SPACECRAFT charging has been the cause of a number of significant anomalies in high-altitude (i.e., geosynchronous) spacecraft as well as the loss of at least one satellite.¹ Concern about these occurrences has led to a number of investigations, including the launch of the Spacecraft Charging at High Altitude (SCATHA) satellite, which was entirely devoted to the study of spacecraft charging. However, little effort has been devoted to the study of high-level charging in low Earth orbit because of the rarity of its occurrence. We report the occurrence of an anomaly associated with high-level surface charging on the low-altitude Defense Meteorological Satellite Program (DMSP) F13 spacecraft. To our knowledge, this is the first published report of the observation of an anomaly associated with spacecraft charging in low Earth orbit. We present data from the environmental sensors aboard the F13 spacecraft that clearly indicate that the spacecraft frame began charging a few seconds prior to the anomaly. We calculate the capacitance of the thermal blankets covering much of the surface of the spacecraft and show that they could easily charge to breakdown voltage within the few seconds prior to the anomaly. Subsequent discharge would have led to electrical breakdown and the observed anomaly.

Charging Background

An orbiting spacecraft is immersed in a plasma that consists of free electrons and ions. These electrons and ions impinge on the spacecraft surface and therefore constitute negative and positive currents to the spacecraft. Other current sources include precipitating energetic electrons and ions, photoelectrons kicked off the spacecraft by ultraviolet photons from the sun, and secondary electrons produced by energetic particle impact with the spacecraft surface. The spacecraft charges to the voltage at which all of the currents

balance to zero. In low Earth orbit, such as the DMSP orbits at ~ 840 km, the plasma density is usually high and the main contributors to these currents are the thermal electrons and ions that constitute the ionosphere. Because the electron thermal velocity is much larger than the thermal velocity of the ions, the electron flux (or current) to the spacecraft is much larger than the ion flux, and the spacecraft charges to some negative potential, usually around -1 V.

When the plasma density is very low, however, the contribution to the currents to the spacecraft from other sources can become very important. In fact, the spacecraft can charge to high negative voltages during times when the plasma density is very low and the flux of energetic electrons is very high. Gussenhoven et al.² showed that the DMSP F6 and F7 spacecraft charged to voltages < -100 V when the following conditions were met: 1) the spacecraft was in darkness, 2) the plasma density was less than 10^4 cm^{-3} , and 3) there was a high integral number flux ($> 10^8$ electrons $\text{cm}^{-2} \text{s}^{-1} \text{sr}^{-1}$) of high-energy (> 14 keV) electrons.

Spacecraft and Instrumentation

The DMSP spacecraft are a series of low-altitude, polar-orbiting, sun-synchronous satellites whose primary mission is to observe the tropospheric weather. Their secondary mission is to observe the space environment using a set of three instruments: the special sensor for ions, electrons, and scintillation (SSIES), the precipitating energetic particle spectrometer (SSJ/4), and the vector magnetometer (SSM). The SSIES measures the in situ ion and electron temperatures, and the plasma density, fluctuations, composition, and bulk flow velocity. The SSJ/4 measures precipitating energetic electrons and ions in the energy range from 30 eV to 32 keV with downward flight paths within a few degrees of local vertical. The SSM measures the strength and direction of the geomagnetic field from which a model field is subtracted to obtain the magnetic-field variations produced by field-aligned currents.

The DMSP F13 spacecraft configuration is shown in Fig. 1. It consists of a honeycomb aluminum, five-sided equipment support

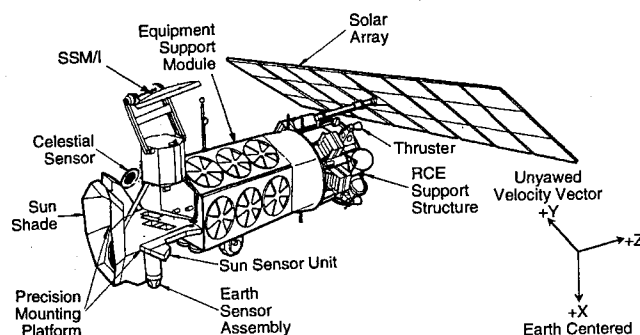


Fig. 1 On-orbit configuration of the DMSP F13 spacecraft.

Received Oct. 1, 1995; revision received April 11, 1996; accepted for publication May 21, 1996. Copyright © 1996 by the American Institute of Aeronautics and Astronautics, Inc. All rights reserved.

*Member, Technical Staff, Space and Environment Technology Center, P.O. Box 92957.

†Senior Scientist, Space and Environment Technology Center, P.O. Box 92957. Member AIAA.

module (ESM) with the solar array at one end and a precision mounting platform at the other end where the microwave imager (SSM/I) is located. The spacecraft coordinate system is shown at the bottom right: *X* is positive toward the center of the Earth, *Y* is in the spacecraft velocity vector direction, and *Z* is along the longitudinal axis of the spacecraft, positive toward the solar array. The ESM is covered with thermal blankets, and pinwheel thermal louvers are used on all but the +*X* side (the side facing the Earth). The SSJ/4 and SSIES instruments are located on the +*Y* side of the ESM near the −*Z* end of the spacecraft; the SSJ/4 looks in the −*X* direction, and the SSIES looks in the +*Y* direction.

Environmental Data

Figure 2 shows the orbital track of the F13 spacecraft around the time at which the anomaly occurred, plotted on a polar dial in invariant latitude (ILAT, a form of magnetic latitude) and magnetic local time (MLT). The spacecraft was in the southern hemisphere moving from dawn to dusk and skimming the inner edge of the polar cap. The lockup occurred at 76° ILAT and 20.33 MLT [21:32:20 universal time (UT)] at the location identified by the large asterisk.

Figures 3a–3d show the electron flux for three energies, 31.3, 9.64, and 2.99 keV, and the ion densities, measured between 21:30 and 21:40 UT while the spacecraft was traversing the nightside auroral zone. The arrows in each figure indicate the time of the SSM/I lockup. The horizontal lines indicate the number flux of high-energy electrons required by Gussenhoven et al.² for high-level charging. F13 entered the evening-side auroral zone near 21:32:20 UT and exited just before 21:38 UT. The spacecraft remained in darkness the entire time. The lockup, at the time shown by the arrows in the figures, occurred during the density depletion between about 21:32:20 and 21:33:15 UT when the density dropped well below 10^2 cm^{-3} , and within the intense electron precipitation at the poleward edge of the evening-side auroral zone between about 21:32:10 and 21:32:20 UT. The electron number flux exceeded $10^8 \text{ electrons cm}^{-2} \text{ s}^{-1} \text{ sr}^{-1}$ several times in the energy channels less than 10 keV, including in the 2.99-keV energy channel within the second density depletion. However, the number flux in the 31.3-keV energy channel exceeded $10^8 \text{ electrons cm}^{-2} \text{ s}^{-1} \text{ sr}^{-1}$ only at the time of the lockup, at which time it was greater than $10^9 \text{ electrons cm}^{-2} \text{ s}^{-1} \text{ sr}^{-1}$.

Four 1-s electron spectra are shown in Figs. 4a–4d. The first spectrum was acquired at 21:32:28 UT, 12 s before the lockup, and displays a typical Maxwellian distribution with a peak near 3 keV. The electrons below about 500 eV are secondary electrons produced by impact of the precipitating energetic electrons with the neutral atmosphere and the spacecraft surface. By 21:32:35 UT, the peak had increased to about 14 keV. At the time of the lockup, 21:32:40 UT, the peak was greater than 31 keV, as indicated by

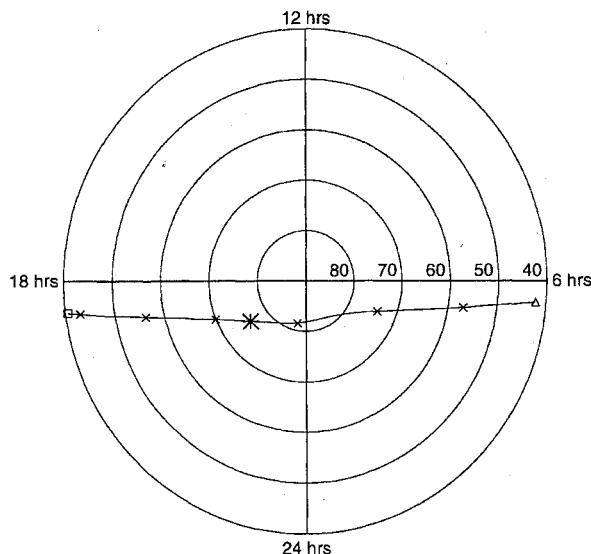


Fig. 2 Spacecraft orbital track in magnetic local time and invariant latitude from 21:16:00 to 21:46:00 UT. ×, 5 min mark; Δ, start of pass; □, end of pass; and *, spacecraft location at time of anomaly.

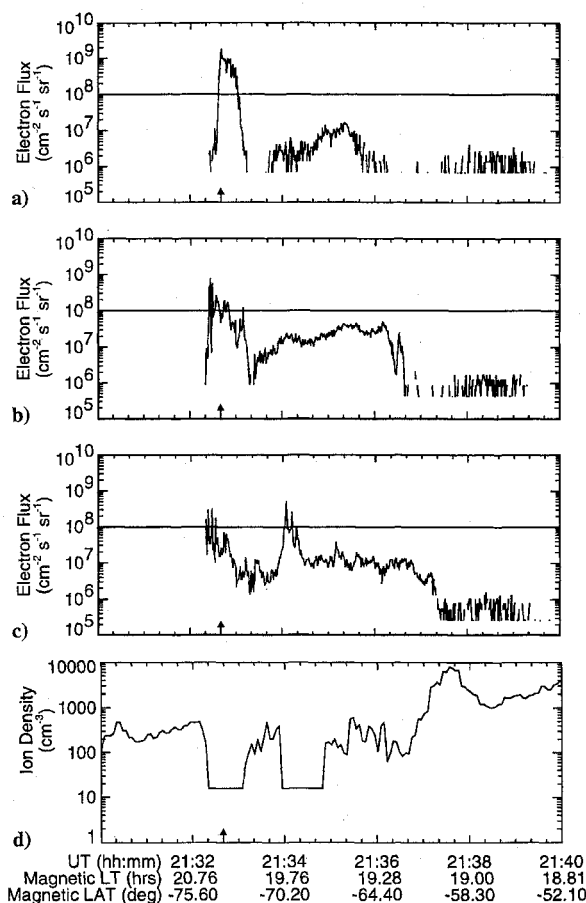


Fig. 3 Electron number fluxes measured by the SSJ/4 in the energy channels: a) 31.3 keV, b) 9.64 keV, c) 2.99 keV, and d) ion density measurements from the SSIES.

the increasing fluxes up to the highest energy channel at 31.3 keV. The peak remained high for several seconds after the lockup as exemplified by the spectrum acquired 3 s later (Fig. 4d).

These data indicate that conditions met the requirements for a high-level charging event on the F13.² The spacecraft was in darkness, the plasma density was well below 10^4 cm^{-3} , and there was a high flux of energetic electrons ($2.0 \times 10^9 \text{ electrons cm}^{-2} \text{ s}^{-1} \text{ sr}^{-1}$ at 31.3 keV and increasing to higher energies). Calculation of the currents to the spacecraft based on the data from the environmental sensors show that the current from the precipitating electrons was much larger than the currents from the thermal electrons and ions. Use of 10^2 cm^{-2} for the thermal electron and ion densities (an upper limit) gives a thermal ion current of $1.2 \times 10^{-9} \text{ A/m}^2$ and a thermal electron current of $8.5 \times 10^{-8} \text{ A/m}^2$. Calculation of the electron current from the precipitating electrons using the SSJ/4 data at the time of the anomaly gives a value of $4.8 \times 10^{-6} \text{ A/m}^2$ (a lower limit because of the SSJ/4 cutoff at 31.3 eV). Thus, the precipitating electron currents were much larger than the thermal currents, and it is expected that the spacecraft would have charged to some large negative voltage. We note that the requirement that the spacecraft be in darkness is not important in this case because the photoelectron current density yield for Teflon® (the outer surface of the thermal blankets, discussed later) is on the order of 10^{-9} A/cm^2 .

A clear indication that the spacecraft frame charged up can be seen in the ion spectra shown in Figs. 5a–5d. These were acquired at the same time as the electron spectra in Figs. 4a–4d. The first spectrum at 21:32:28 UT is a typical ion spectrum with two peaks, similar to the electron spectrum. Starting at 21:32:35 UT, there was a dramatic increase in the number flux in the 144-eV channel, but there were no ions at lower energies. These measurements indicate that the voltage on the SSJ/4 sensor aperture, which is the same as the voltage on the spacecraft frame, became about 144 V. All of the thermal ions (which have energies less than 1 eV) were accelerated to 144 eV as they passed through the plasma sheath in front of the aperture. The energy channel with the peak number flux at the time of the

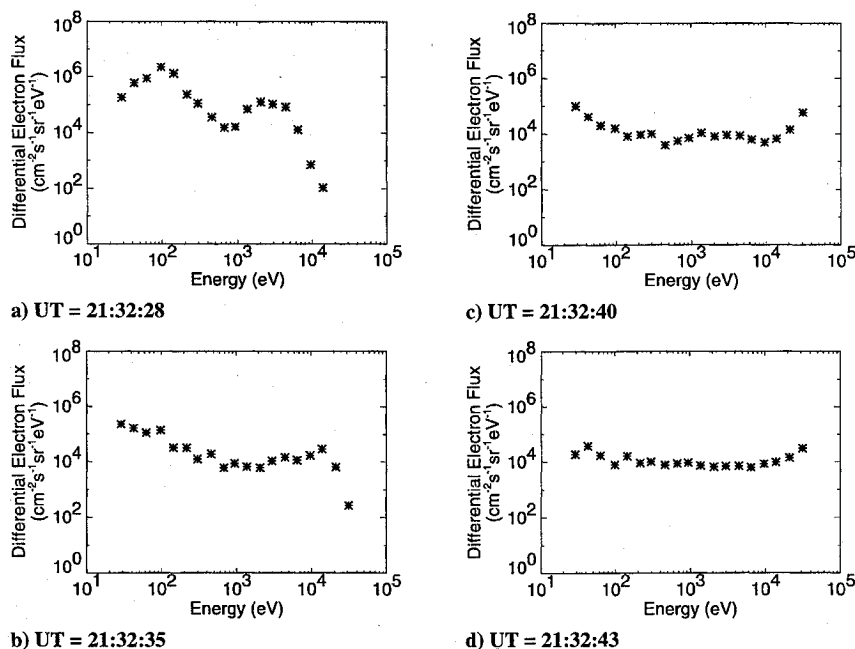


Fig. 4 Electron spectra measured by the SSJ/4 for four different 1-s periods.

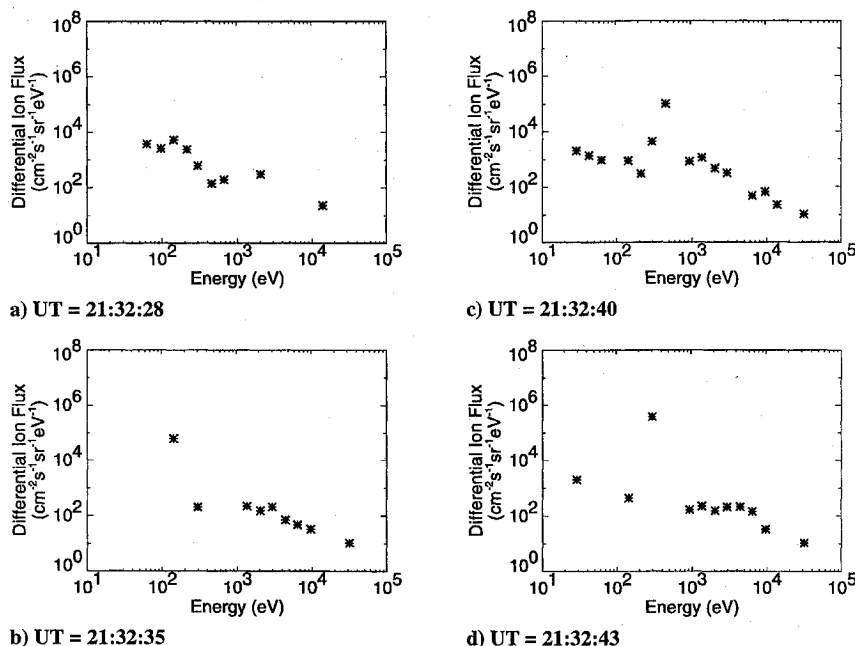


Fig. 5 Ion spectra measured by the SSJ/4 for the four 1-s periods of Figs. 4a–4d.

lockup, 21:32:40 UT, was 459 eV indicating that the spacecraft frame charged up to near 459 V. (The ion counts seen at lower energies during the charging are contamination from the high-energy electrons.) It remained charged for several seconds after the lockup as evidenced by the ion spectrum at 21:32:43 UT.

Electrostatic Discharge

The deposition of charge in dielectric materials by energetic particles is a known source of spacecraft charging.^{3–5} Electrons between 10 and 100 keV lose energy at a rate $R = 10^6$ to 5×10^7 eV cm² g⁻¹ depending on the electron energy and material involved.⁶ The energy loss per centimeter is given by $R \cdot \rho$; therefore the incident energetic electrons penetrate the material to a depth of a few microns, where they form a space-charge layer. This charge builds up until a critical value is reached, wherein a breakdown occurs that is accompanied by material vaporization and ionization. A discharge is initiated that propagates across the surface or through

the material, removing part of the bound charge. These discharges typically occur in holes, cracks, seams, or edges of the material and have been known to seriously damage spacecraft components. Although they have been studied extensively in high Earth orbit (i.e., geosynchronous),^{3,7,8} none have been observed previously in low Earth orbit because of the normally high background plasma densities.

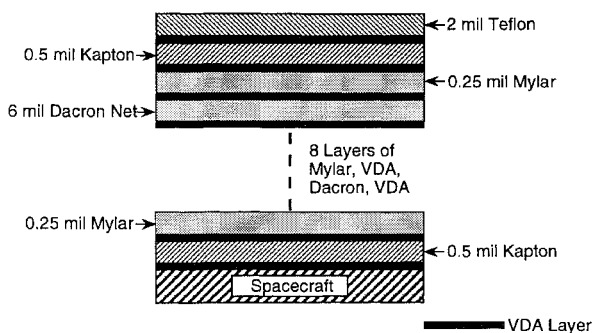
The exposed dielectric surfaces of the spacecraft consist of thermal blankets and pinwheel thermal louvers for thermal control of the spacecraft. The top (–x) two surfaces of the ESM are covered with the thermal blankets and pinwheel thermal louvers, and the exposed surfaces of the SSM/I are covered with thermal blankets.

Thermal Blankets

Thermal blankets consist of many layers of dielectric material, some coated with vapor-deposited aluminum (VDA). The thermal blankets covering the top surfaces of the DMSP F13 spacecraft

Table 1 Dielectric materials composing the DMSP thermal blankets

Dielectric material	Number of layers	Layer thickness, mil	Effective dielectric constant
Teflon	1	2.0	2
Kapton	2	0.5	3.4
Mylar	10	0.25	2
Dacron mesh	9	6.0	1

**Fig. 6 Layered structure of the thermal blankets.**

consist of 22 layers of material as shown in Fig. 6. All of the Kapton[®] and Mylar[®] layers are aluminized on both sides, whereas the outer Teflon layer is aluminized only on the side facing the spacecraft. Blanket assembly and attachment were accomplished using urethane tacks, Nomex Velcro[®] zippers, and tapes. Because the intermediate layers of the thermal blankets are not grounded to the spacecraft frame, the VDA coatings serve as the plates of a set of 22 parallel-plate capacitors in series. The top plate consists of the electrons buried in the top few microns of the Teflon and the bottom plate is the layer of VDA that is in contact with the spacecraft frame. The materials composing the various layers of the thermal blankets and their dielectric properties are shown in Table 1. The effective dielectric constant for the Dacron[®] mesh is taken to be 1 because the mesh has a very open weave. Using the values in the table, we calculate the total capacitance for the blankets to be 7.3×10^{-9} F/m².

The time to charge the outer surface of a parallel-plate capacitor to some voltage with respect to the spacecraft frame is given by

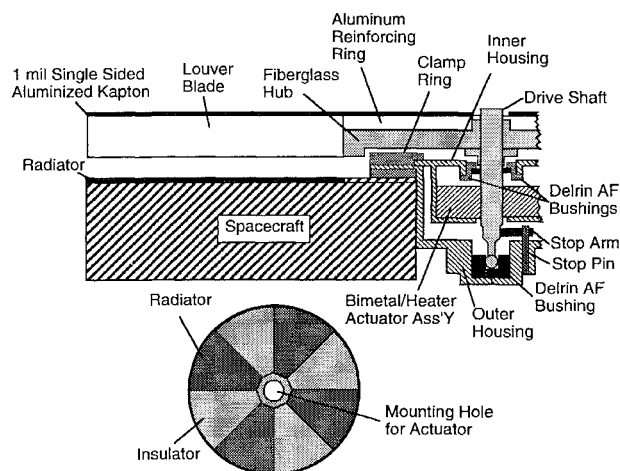
$$t = \frac{CV}{i(1-\delta)A} \quad (1)$$

The secondary electron yield δ is defined as the ratio between the total number of emitted electrons and the total number of primary or incident electrons. For Teflon at 30 keV, $\delta \approx 0.2$. This effectively reduces the charging current and increases the charging time.

Laboratory measurements have shown that Teflon will discharge at 3 kV in a 20-keV electron beam.⁹ Using the measured incident precipitating electron current density of 4.8×10^{-6} A/cm² in the aurora, the charging time calculated from Eq. (1) for the thermal blanket to reach 3 kV is about 5.7 s. Because the measured current was a lower limit on account of the lack of electron measurements beyond 32 keV, 5.7 s is an upper limit on the charging time. This is on the order of the time it took for the DMSP F13 blankets to reach breakdown voltage under the conditions encountered on May 5, 1995.

Pinwheel Thermal Louvers

The pinwheel thermal louvers mounted on the top two sides cover a considerable fraction of the spacecraft surface. Each consists of a rotatable four-lobed louver blade mounted approximately 0.64 cm above a special radiator pattern. A cutaway diagram of the thermal louvers is shown in Fig. 7 along with a top view of the radiator pattern. The louver blades are composed of several layers of dielectric materials and the radiator pattern consists of alternating segments of aluminized Teflon (radiator) and fiberglass-reinforced aluminized Kapton (insulator). The blades cover the Teflon areas when in the closed position and cover the Kapton areas when in the open position, and so, the louver blades cover half of the radiator pattern at any given time. The insulator sections consist of 10 mil of

**Fig. 7 Structure of the pinwheel thermal louvers: radiator pattern.**

aluminized Teflon bonded to the ESM panel, whereas the radiator sections consist of 1 mil of aluminized Kapton on top of 9 mil of fiberglass bonded to the ESM panel. Thus the capacitance for the exposed segments of the radiator pattern at any given time is much larger than for the thermal blankets: 7.0×10^{-8} F/m² for the radiator and 1.8×10^{-7} F/m² for the insulator. Therefore the time to charge those exposed segments of the radiator pattern is much larger than that for the thermal blankets.

The pinwheel activator assembly (Fig. 7) consists of a drive-shaft assembly, two Delrin AF[®] (an insulating plastic) bushings, a bimetallic element and housing, an outer housing, and a clamp ring. The drive-shaft assembly is attached to the inner coil of the bimetallic element and carries the stop arm and two bearing surfaces, which ride in the Delrin AF bushings, one of which is mounted in the bimetallic housing. The bimetallic housing mounts inside the outer housing, which contains the stop element and an adjustable Delrin AF bushing. The entire assembly mounts in a hole in the ESM panel and is held in place with a clamp ring.

The blade assembly consists of a hub, foam sandwich blades, and a single-sided aluminized Kapton outer shield. The outer shield is bonded at the hub to an aluminum reinforcing ring on top of single-sided aluminized fiberglass. The hub is then attached to the drive shaft. The capacitance of this assembly is obviously much more complicated to calculate than the capacitance of the thermal blankets. However, the only possible path for a discharge is from the Kapton outer shield through the aluminum reinforcing ring, down the shaft, and across the Delrin AF bushings (or across the stop arm and stop pin if they are in contact). Thus a discharge would occur within the actuator casing well removed from the SSM/I. A much more probable location for the discharge is on the thermal blankets surrounding the SSM/I or on one of the top two ESM panels, particularly as we have shown that the time for the thermal blankets to reach discharge voltage is on the order of the charging time indicated by the environmental data. There are several high-impedance lines running to the SSM/I from other places on the spacecraft that could have conducted an electrostatic pulse from a discharge into the microprocessor.

Discussion

The occurrence of large fluxes of high-energy electrons is not a rare event in the aurora, and the driving factor that led to the spacecraft charging on the DMSP F13 satellite on May 5, 1995, was the low-density region accompanying the aurora. Ionospheric densities are generally related to solar activity with densities being much less at DMSP altitudes (by about a factor of 10) during solar minimum than at solar maximum. We are currently entering the minimum of the 11-year solar cycle and the study of Gussenhoven et al.² was performed in 1983, prior to the previous minimum, when they recorded several incidents of high-level charging. They did not report any anomalies, but we would note that the F6 and F7 spacecraft had a different configuration and lacked an SSM/I. There are plans to raise the DMSP spacecraft orbit to a higher altitude

where the plasma densities would be even lower and could lead to greater incidents of high-level charging.

If the VDA layer on the bottom side of the outer Teflon were grounded to the spacecraft frame, the capacitance of the Teflon layer would be the entire capacitance to be charged by the auroral electrons. The capacitance of that single layer would be much higher than the capacitance of all of the ungrounded layers in series as configured in the original blanket. The capacitance of a 2-mil Teflon-filled capacitor is 3.5×10^{-7} F/m². The charging time to 3000 V, calculated from Eq. (1), would then be 132 s, and the thermal blankets would not have enough time to reach breakdown voltage during the time it takes the spacecraft to cross the auroral region. Thus increasing the capacitance of the thermal-blanket outer layer is an effective method for mitigating against surface discharges on low-altitude spacecraft.

This technique should not be used on high-altitude spacecraft traversing the plasma sheet because they are exposed to the charging environment there for much longer than 132 s and would still be expected to reach breakdown voltage. The resulting discharge would be larger if the capacitance of the blanket were increased.

Conclusions

We have determined that the SSM/I lockup is consistent with an electrostatic discharge occurring on the spacecraft because of differential charging of the dielectric surfaces (i.e., the thermal blankets). The evidence from the environmental sensors is very clear. The spacecraft frame began charging about 5 s before the lockup, was charged to about 459 V by the time of the lockup, and remained charged for several seconds. Capacitance and surface-charging time calculations indicate that the surface of the thermal blankets would charge to 3 keV or higher within about 5 s. A subsequent discharge is likely to have caused the lockup in the SSM/I. We cannot determine where on the spacecraft the discharge (or discharges) occurred; however, there are several high-impedance lines running to the SSM/I from other places on the spacecraft that could have conducted an electrostatic pulse from a discharge into the microprocessor. A simple fix would be to ground the aluminum layer on the bottom of

the top Teflon layer to the spacecraft frame because the energetic electrons do not penetrate beyond this layer.

Acknowledgments

This work was supported by the Space and Missile Systems Center of the U.S. Air Force under Contract F04701-88-C-0089. The authors would like to thank F. Rich for providing the DMSP F13 data used in this study.

References

- ¹Shaw, R. R., Nanevicz, J. E., and Adamo, R. C., "Observations of Electrical Discharges Caused by Differential Satellite Charging," *Spacecraft Charging by Magnetospheric Plasma*, edited by A. Rosen, Vol. 47, Progress in Astronautics and Aeronautics, AIAA, New York, 1976, pp. 61-76.
- ²Gussenhoven, M. S., Hardy, D. A., Rich, F., Burke, W. J., and Yeh, H.-C., "High Level Charging in the Low-Altitude Polar Auroral Environment," *Journal of Geophysical Research*, Vol. 90, No. A11, 1985, pp. 11,000-11,023.
- ³De Forest, S. E., "Spacecraft Charging at Synchronous Orbit," *Journal of Geophysical Research*, Vol. 77, No. 5, 1977, pp. 651-659.
- ⁴Mizera, P. F., "First Results of Material Charging in the Space Environment," *Applied Physics Letters*, Vol. 37, No. 3, 1980, pp. 276-279.
- ⁵Lueng, M. S., and Kan, H. K. A., "Laboratory Study of the Charging of Spacecraft Materials," *Journal of Spacecraft and Rockets*, Vol. 18, No. 6, 1981, pp. 510-514.
- ⁶Fredrickson, A. R., "Radiation Induced Dielectric Charging," *Space Systems and Their Interactions with the Earth's Space Environment*, edited by H. B. Garrett and C. P. Pike, Vol. 71, Progress in Astronautics and Aeronautics, AIAA, New York, 1980, pp. 386-412.
- ⁷Koons, H. C., Mizera, P. F., and Fennell, J. F., "Spacecraft Charging Results from the SCATHA Satellite," *Astronautics and Aeronautics*, Vol. 18, No. 11, 1980, pp. 44-47.
- ⁸Rubin, A. G., and Garrett, H. B., "ATS-5 and ATS-6 Potentials During Eclipse," *Spacecraft Charging Technology Conference, 1978*, edited by R. C. Finke and C. P. Pike, AFGL-TR-79-0082/NASA-CP-2071, 1979, pp. 38-43.
- ⁹Plamp, G., private communication, Lockheed Martin Corp., Denver, CO, April 1995.

H. R. Anderson
Associate Editor